Space/Time Multipath Separation and Equalization in Asynchronous CDMA using the Spatio-Temporal Array-Receiver

Sofiène AFFES and Paul MERMELSTEIN

INRS-Télécommunications, Université du Québec
16, Place du Commerce, Ile des Soeurs, Verdun, QC, H3E 1H6, Canada
Tel: (1) (514) 765.7817/7769 - Fax: (1) (514) 761.8501
E-mail: affes,mermel@inrs-telecom.uquebec.ca

Abstract— ***We propose a spatio-temporal array-receiver for asynchronous CDMA using a new space/time structural approach. First, STAR performs blind identification and equalization of the propagation channel from each mobile transmitter. Second, it provides fast and accurate estimates of the number, relative magnitude and delay of the multipath components. From this space/time separation, we reconstruct the identified channel with respect to a partially revealed space/time structure and reduce identification errors by an order of the processing gain over the number of paths. Simulations confirm good multipath acquisition properties of STAR in the presence of strong interference and fast Doppler.***

I. Introduction

Array processing was recently applied to synchronous CDMA [1] to improve the capacity of personal communication systems. Its exploitation motivates the development of new multi-user access methods for asynchronous CDMA [2]-[4]. Most of these techniques (*e.g.*, [2],[3]) efficiently address processing in space for combining multipath and antenna diversity branches. They involve however separate processing in time for synchronization and sampling following the classical RAKE structure [1]. Therefore, time-acquisition is still subject to potential improvements.

Blind multi-channel identification or equalization methods which propose joint space-time processing offer a good alternative to the RAKE, but they have been usually applied in TDMA (see the survey and references in [5]). Recently, some blind multi-channel equalization schemes were proposed in CDMA (*e.g.*, [4]). These techniques implicitly perform synchronization and array combining by channel equalization in space and time. However, they process the received signals before correlation and do not exploit the particular structure of the despread data in CDMA.

Unlike [4], we consider a blind multi-channel approach over the despread data and develop a novel block-data formulation denoted as the post-correlation model (PCM). This new PCM model characterizes the structure of the channel in space and time and can be interpreted as an instantaneous mixture in a one-dimensional spatio-temporal signal subspace. It allows for use of low complexity narrowband processors.

We propose here the spatio-temporal array-receiver (STAR). By an adaptive subspace-tracking procedure, STAR first achieves blind identification and equalization of the channel and implicitly performs integrated and efficient multipath capture and combining in one step. Second, contrary to [4], it exploits the known structure of the identified channel in time and proposes a new localization procedure for estimating the number of paths and their time-delays. Such time characterization was recently considered in [6]-[9] for other applications than CDMA following different approaches. Here it achieves a space/time separation of the identified channel. Channel reconstruction from this space/time decomposition reduces identification errors by an order of the processing gain over the number of multipaths, and significantly improves the performance of the algorithm.

Two localization options for STAR are considered. The first, STAR-SS, performs localization by "source"-structure analysis. It is very fast and more efficient for slow Doppler. The second, STAR-ES, performs localization by eigen-structure analysis. It is slower and more complex, but more accurate and efficient for fast Doppler.

STAR finally offers an attractive and simple structure with a very low complexity. Simulations confirm its effectiveness and its multipath acquisition capability at high interference levels and over a wide range of Doppler.

II. New Block Formulation and Spatio-Temporal Modeling

We consider a cellular CDMA system where each base-station is equipped with a receiving antenna of M sensors. The BPSK bit sequence of the desired user is first differentially encoded at the rate $1/T$, where T is the bit duration. The resulting DBPSK sequence $b(t)$ is then spread by a periodic personal code $c(t)$ at the rate $1/T_c$, where T_c is the chip pulse duration. The period of $c(t)$ is assumed to be equal to the bit duration T, although the results can be adequately extended to code periods that are multiples of T. The processing gain is given by $L = T/T_c$. We also assume a multipath fading environment where the number of paths P is unknown and where the time-delay spread is small compared to T.

At time t, the observation vector received by the antenna array can be written as follows:

$$X(t) = \psi(t) \sum_{p=1}^{P} G_p(t)\varepsilon_p(t)b(t-\tau_p)c(t-\tau_p) + \mathcal{I}(t) \ , \quad (1)$$

where $\tau_p \in [0, T[$ are the propagation time-delays along the P paths, $p = 1, \cdots, P$, and $G_p(t)$ are the propagation vectors with an equal norm to be fixed later. $\varepsilon_p^2(t)$ are the fractions (*i.e.*, $\sum_{p=1}^{P} \varepsilon_p^2(t) = 1$) of the total power

0-7803-3777-8/97/$10.00 © 1997 IEEE

$\psi^2(t)$ received from the desired user along each path. The received power estimation includes the effect of path loss and shadowing. We assume very slow and locally constant time-variations of $G_p(t)$, $\varepsilon_p^2(t)$ and $\psi^2(t)$, as compared to the bit duration T. The noise term $\mathcal{I}(t)$ includes the thermal noise received at the antenna elements and the total received interference. For the sake of simplicity, the time-delays are assumed constant in this paper. The tracking of time-varying multipath delays is addressed in [10].

At successive frames of period T, we now define over the time-interval $[0, T[$ the post-correlated observation vector of the frame number n by:

$$Z_n(t') = \frac{1}{T}\int_0^T X(t+t'+nT)c(t)dt \qquad (2)$$
$$\simeq b(nT)\psi(nT)\sum_{p=1}^{P} G_p(nT)\varepsilon_p(nT)\rho_c(t'-\tau_p)+N_n(t'),$$

where $\rho_c(t')$ is the correlation function of the chip pulse and $N_n(t')$ is the post-correlation noise of the frame[1] number n. Since the chip pulse is time-limited to $[0, T_c]$, its auto-correlation function $\rho_c(t')$ is null for $|t'| \geq T_c$ and time-limited to $t' \in [-T_c, T_c]$. Over the p^{th} path, $\rho_c(t'-\tau_p)$ can be seen for $t' \in [0, T[$ as a time-delayed impulse response[2] observed at the frequency resolution $1/T_c$.

For each frame, we sample $Z_n(t')$ for $t' \in [0, T[$ at the chip rate $1/T_c$ and form the $M \times L$ block data matrix denoted by $\mathbf{Z}_n = [Z_n(0), Z_n(T_c), \cdots, Z_n((L-1)T_c)]$ and referred to as the post-correlated observation matrix. Using Eq. (2), $\mathbf{Z}_n$ can be explicitly written as follows:

$$\mathbf{Z}_n = b_n\psi_n\sum_{p=1}^{P} G_{p,n}\varepsilon_{p,n}D_p^T + \mathbb{N}_n \qquad (3)$$
$$= b_n\psi_n\mathbf{G}_n\Upsilon_n\mathbf{D}^T + \mathbf{N}_n \ ,$$

where b_n, ψ_n, $G_{p,n}$ and $\varepsilon_{p,n}$ are respectively equal to $b(nT)$, $\psi(nT)$, $G_p(nT)$ and $\varepsilon_p(nT)$; $\mathbf{G}_n = [G_{1,n}, \cdots, G_{P,n}]$ is the propagation matrix, $\Upsilon_n = \text{diag}\{[\varepsilon_{1,n}, \cdots, \varepsilon_{P,n}]\}$ is the diagonal matrix of power partition over multipaths. Finally, $\mathbf{N}_n = [N_n(0), N_n(T_c), \cdots, N_n((L-1)T_c)]$ is the noise matrix, and $\mathbf{D} = [D_1, \cdots, D_P]$ is the time response matrix where $D_p = [\rho_c(-\tau_p), \rho_c(T_c-\tau_p), \cdots, \rho_c((L-1)T_c-\tau_p)]^T$ is the time-delay impulse response of τ_p sampled at $1/T_c$. Its column-by-column FFT is $\mathcal{D} = [\mathcal{D}_1, \cdots, \mathcal{D}_P]$ and its columns belong to a time manifold say $\mathbb{\Gamma}$[3]:

$$\mathcal{D}_p = \mathcal{F}(\tau_p) \in \mathbb{\Gamma} \quad \text{for} \quad p = 1, \cdots, P \qquad (4)$$
$$= \left[1, e^{-j2\pi\tau_p\frac{1}{L}}, \cdots, e^{-j2\pi\tau_p\frac{L-1}{L}}\right]^T .$$

[1] In Eq. (2), the frame edges should not lie in the middle of the delay spread. Such an event could be detected from the localization results. In this particular case, we either run a parallel version or restart the algorithm with the data delayed by $T/2$. For a large delay spread, we should consider multiples of T code periods. This issue is presently under study.

[2] It may be required here to design pulses whose correlation is very close to a sinc function, but the approximation holds in general.

[3] In [8],[9], the pulse function modulating symbols is included in the time manifold. Similarly, it is the exact correlation function of the chip code $\rho_c(t)$ that could be included here, but the approximation made with simple delays is satisfying in the CDMA context.

For the sake of simplicity, we may equivalently say that $\mathbf{D}$ or $\mathcal{D}$ belongs to the manifold $\mathbb{\Gamma}$ without distinction. Later, we shall use this feature to implement the time-delays acquisition step.

We now rewrite Eq. (3) in the following compact form:

$$\mathbf{Z}_n = \mathbf{H}_n s_n + \mathbf{N}_n \ , \qquad (5)$$

where $\mathbf{H}_n = \mathbf{G}_n\Upsilon_n\mathbf{D}^T = \mathbf{J}_n\mathbf{D}^T$ is the spatio-temporal propagation matrix and $s_n = b_n\psi_n$ is the signal component. Notice here that while the columns of the time response matrix $\mathbf{D}$ are defined in the manifold $\mathbb{\Gamma}$, the spatial response matrix $\mathbf{J}_n = \mathbf{G}_n\Upsilon_n$ is not modeled[4] and defines the unknown part of the spatio-temporal structure of $\mathbf{H}_n$.

Eq. (5) provides a new instantaneous mixture model at the bit rate where the signal subspace covers a one-dimensional $M \times L$ matrices space. The matrices $\mathbf{Z}_n$,$\mathbf{H}_n$ and $\mathbf{N}_n$ are transformed into $(M \times L)$-dimensional vectors by arranging their columns as one spatio-temporal column vector to yield:

$$\underline{\mathbf{Z}}_n = \underline{\mathbf{H}}_n s_n + \underline{\mathbf{N}}_n \ , \qquad (6)$$

where $\underline{\mathbf{Z}}_n$, $\underline{\mathbf{H}}_n$ and $\underline{\mathbf{N}}_n$ respectively denote the resulting vectors. To avoid the ambiguity due to any multiplicative factor between $\underline{\mathbf{H}}_n$ and s_n, we fix the norm of $\underline{\mathbf{H}}_n$ to $\sqrt{M}$. As mentioned earlier, the norm of propagation vectors $G_{p,n}$ is implicitly fixed to the same value say $\sqrt{K_n}$ for $p = 1, \cdots, P$ in such a way that $\|\underline{\mathbf{H}}_n\|^2 = M$. We will explicitly give its expression later.

What it is original about the new data block model is that the signal component s_n is a scalar and that the spatio-temporal signal subspace generated by the the space-time propagation vector $\underline{\mathbf{H}}_n$ is one-dimensional. It is the correlation step that almost cancels ISI and that allows for such a model, contrary to recent blind methods in CDMA (*e.g.*, [4]) that process the data before correlation following the new blind multi-channel approaches (see the survey in [5]). Therefore, this original post-correlation model (PCM) permits any low complexity narrowband array processing technique to be used. In particular, eigen-subspace tracking or principal component analysis methods could be used to identify $\underline{\mathbf{H}}_n$ in a blind approach. From that estimate, narrowband array beamformers could be used to estimate s_n in a blind space-time equalization-like step.

Using Eq. (6) next, we first propose a spatio-temporal identification and equalization procedure adapted from [11] for simultaneously estimating $\underline{\mathbf{H}}_n$ and s_n. Second, in Eq. (5), we achieve a space/time structural separation and reconstruction of the identified channel (*i.e.*, $\mathbf{H}_n = \mathbf{J}_n\mathbf{D}^T$). This step captures multipath delays, reduces identification errors by a factor of L/P and improves the performance of STAR as shown later. Finally, both steps can be permanently combined in one step for multipath tracking as explained in [10].

[4] We may characterize $\mathbf{G}_n$ in a space manifold parameterized by angles of arrivals as in [7]-[9]. However, a space characterization is often much more restrictive than a time characterization. Besides, it requires perfect antenna calibration and adequate sensor positioning.

III. The Proposed Structure of STAR

A. Spatio-Temporal Identification and Equalization

We first assume that an estimate of $\underline{\underline{\mathrm{H}}}_n$ say $\underline{\underline{\tilde{\mathrm{H}}}}_n$ is available at each block iteration n [11]. From this estimate, we can extract the signal component s_n by any-distortionless beamformer W_n (*i.e.*, $W_n^H \underline{\underline{\tilde{\mathrm{H}}}}_n = 1$). It is reasonable to assume that $\underline{\mathrm{N}}_n$ is an uncorrelated white noise vector so that a Delay-Sum (DS) beamformer (*i.e.*, $W_n = \underline{\underline{\tilde{\mathrm{H}}}}_n / M$) is optimal for source extraction [11]. This beamformer achieves a spatio-temporal blind equalization by matched filtering in an $M \times L$ dimensional space, and estimates s_n by:

$$\hat{s}_n = \mathrm{Real}\left\{W_n^H \underline{\mathrm{Z}}_n\right\} = \mathrm{Real}\left\{\underline{\underline{\tilde{\mathrm{H}}}}_n^H \underline{\mathrm{Z}}_n / M\right\}, \tag{7}$$

where the Real{.} function extracts the real signal component sequence $s_n = \psi_n b_n$ and further reduces the noise by half [11]. From this estimate, the total power received from the desired user is estimated for power control by:

$$\hat{\psi}_n^2 = (1-\alpha)\ \hat{\psi}_{n-1}^2 + \alpha\ |\hat{s}_n|^2, \tag{8}$$

where $\alpha \ll 1$ is a smoothing factor (see [11] for more details), while the bit sequence $\hat{b}_n$ is estimated as the sign of $\hat{s}_n$. We finally track $\underline{\underline{\mathrm{H}}}_n$ in a blind identification scheme by the following simple and fast LMS-type subspace-tracking procedure [11]:

$$\underline{\underline{\tilde{\mathrm{H}}}}_{n+1} = \underline{\underline{\tilde{\mathrm{H}}}}_n + \mu_n (\underline{\mathrm{Z}}_n - \underline{\underline{\tilde{\mathrm{H}}}}_n \hat{s}_n) \hat{s}_n^H, \tag{9}$$

where μ_n is an adaptation step-size possibly normalized. Notice that $\hat{b}_n \hat{\psi}_n$ can be used instead of $\hat{s}_n$. This equation converges to $\underline{\underline{\mathrm{H}}}_n$ with norm $\sqrt{M}$ within a sign ambiguity (*i.e.*, $\underline{\underline{\tilde{\mathrm{H}}}}_n \simeq \pm \underline{\underline{\mathrm{H}}}_n$ when $n \to \infty$) [11]. This ambiguity has no consequences other than changing the signs of $\hat{s}_n$ and $\hat{b}_n$ since b_n is a DBPSK sequence. For the sake of simplicity, we assume in the following that $\underline{\underline{\tilde{\mathrm{H}}}}_n$ converges to $\underline{\underline{\mathrm{H}}}_n$ without loss of generality.

Actually, other eigen-subspace tracking techniques can be used to estimate $\underline{\underline{\mathrm{H}}}_n$. However, what it is original about the identification procedure we proposed in (9) is that it combines eigen-subspace tracking with decision feedback through $\hat{s}_n$ as a reference signal. This decision feedback identification (DFI) feature forces the convergence to $\underline{\underline{\mathrm{H}}}_n$ within a sign ambiguity. It also allows for the reduction of interference by half by taking the real part of the beamformer output in (7). We show in [11] that this DFI feature increases the capacity by a factor of almost 2. Other eigen-subspace tracking techniques estimate $\underline{\underline{\mathrm{H}}}_n$ within a phase ambiguity and have no control over it. Therefore, they cannot achieve that additional gain in capacity.

At this stage, STAR achieves all the required goals. It implicitly synchronizes the data through channel equalization without time-delays acquisition, simultaneously estimates the bit sequence and controls the transmitted power, all at a low order of complexity of $O(ML)$. However, fitting the identified channel with its partially known space/time structure [12] (*i.e.*, $\mathbf{H}_n = \mathbf{J}_n \mathbf{D}^T$ and $\mathbf{D} \in \mathbb{\Gamma}$) significantly reduces identification errors and improves the performance of STAR. We next address this point.

B. Space/Time Structural Separation and Reconstruction

In the following, we propose two time-delay acquisition techniques (*i.e.*, estimation of $\hat{\mathbf{D}} \in \mathbb{\Gamma}$) that can be applied in complementary situations covering both a very wide range of time-variations of the spatial matrix $\mathbf{J}_n$. As explained below, these procedures achieve a "space/time" separation of the spatio-temporal matrix (*i.e.*, estimation of $\hat{\mathbf{J}}_n$) and allow its reconstruction (*i.e.*, $\hat{\mathbf{H}}_n = \hat{\mathbf{J}}_n \hat{\mathbf{D}}^T$ instead of $\tilde{\mathbf{H}}_n$) with a reduction of identification errors by a factor of L/P.

B.1 Source-Structure Time-Delay Acquisition Approach: STAR-SS

Consider the situation where the time-variations of the spatial matrix $\mathbf{J}_n$ are slow enough (this case actually covers the range of Rayleigh Doppler so far considered in cellular CDMA), so that the spatio-temporal identification by Eq. (9) can be made with an acceptable error. Indeed, the time-variations of $\underline{\underline{\mathrm{H}}}_n$ involve those of $\mathbf{J}_n$ which degrade identification as they increase.

Once convergence of $\underline{\underline{\tilde{\mathrm{H}}}}_n$ is reached, we can properly reshape it back into a $M \times L$ matrix and have:

$$\tilde{\mathbf{H}}_n^T = \mathbf{D}\mathbf{J}_n^T + \mathbf{E}_n^T, \tag{10}$$

where $\mathbf{E}_n^T$, the matrix of identification errors, is considered as a low additive noise matrix. Let us then define the column-by-column FFT of $\tilde{\mathbf{H}}_n^T$ by $\tilde{\mathcal{H}}_n = \mathcal{D}\mathbf{J}_n^T + \mathcal{E}_n$, where $\mathcal{E}_n$ denotes the column-by-column FFT of $\mathbf{E}_n^T$. From this equation, the estimation of $\mathcal{D}$ and $\mathbf{J}_n$, which amounts to a "space/time"-like separation, can be achieved in a way similar to source separation. Other techniques [8],[9] rely on a space-time model of the channel similar to Eq. (10), but mainly deal with a 2D localization problem. Here we give a different interpretation of the channel and address the issue of the space/time separation of its structure. With respect to this view, the column vectors of $\tilde{\mathcal{H}}_n$ constitute observation vectors in M parallel spaces, while the column vectors of $\mathbf{J}_n^T$ can be seen as signal vectors of P sources different from one space to another. However, all the sources propagate in the M different spaces along the same trajectories defined by the common propagation matrix $\mathcal{D}$, where the multipath time-delays $\tau_{p,n}$ stand for angles of arrival of plane-wave sources (see Eq. (4)). The manifold $\mathbb{\Gamma}$ contains $\mathcal{D}$ (or $\mathbf{D}$) and can be viewed as an "array" manifold.

Based on the above analogy, $\mathcal{F}(\tau)^H \tilde{\mathcal{H}}_n \tilde{\mathcal{H}}_n^H \mathcal{F}(\tau)/(ML^2)$ can be viewed as an array pattern averaged over sensors. It measures the average energy of $\mathcal{F}(\tau) \in \mathbb{\Gamma}$ that is present in the M parallel source-subspaces and its resolution of the chip pulse duration T_c is sufficient for time-delay localization. We hence define the localization spectrum of STAR-SS in the frequency domain as:

$$\mathcal{S}_{\mathrm{SS}}(\tau) = \frac{1}{1 - \mathcal{F}(\tau)^H \tilde{\mathcal{H}}_n \tilde{\mathcal{H}}_n^H \mathcal{F}(\tau)/ML^2}. \tag{11}$$

This spectrum reveals P peaks at the time-delay locations from which estimates of the number of paths $\hat{P}$ and their time-delays $\hat{\tau}_1, \cdots, \hat{\tau}_{\hat{P}}$ can be obtained.

By analogy to a reference algorithm for source localization, MUSIC [13], we avoid the prohibitive search over the time-delay locations in $[0, T[$ and propose a solution that is similar to root-MUSIC [14]. We define the following $(2L-2)$-degree polynomial:

$$\mathcal{P}_{\text{SS}}(z) = 1 - \mathcal{F}(\tau)^H \tilde{\mathcal{H}}_n \tilde{\mathcal{H}}_n^H \mathcal{F}(\tau)/ML^2, \quad (12)$$

where $z = e^{-j2\pi\frac{\tau}{L}}$. If $\hat{z}_1, \cdots, \hat{z}_{L-1}$ denote the $L-1$ roots in the unit circle of the equation $\mathcal{P}_{\text{SS}}(z) = 0$, then $\mathcal{P}_{\text{SS}}(\hat{z}_1/|\hat{z}_1|), \cdots, \mathcal{P}_{\text{SS}}(\hat{z}_{L-1}/|\hat{z}_{L-1}|)$ reveal the extrema of the spectrum $\mathcal{S}_{\text{SS}}(\tau)$ and give $\hat{P}$ and $\hat{\tau}_1, \cdots, \hat{\tau}_{\hat{P}}$ if we provide them in a decreasing order. Then $\hat{\mathbf{D}}$ is the column-by-column inverse FFT of $\hat{\mathcal{D}} = \left[\mathcal{F}(\hat{\tau}_1), \cdots, \mathcal{F}(\hat{\tau}_{\hat{P}})\right]$.

B.2 Eigen-Structure Time-Delay Acquisition Approach: STAR-ES

Consider now the situation where the time-variations of $\mathbf{J}_n$ are very fast, so that the spatio-temporal identification errors become very high. Then we subject the post-correlated observation matrix $\mathbf{Z}_n^T$ in (5) instead of $\tilde{\mathbf{H}}_n^T$ in (10) to another acquisition approach based on eigen-structure. Here, we exploit new adaptations of MUSIC [13] and of root-MUSIC [14] for a better illustration, but other high resolution techniques such as ESPRIT or the ML approach can be used (see [6]-[9]).

In this approach, we assume uncorrelated multipath fading. Using the same analogy developed earlier, the column vectors of $\mathbf{J}_n^T$ can be again seen as signal vectors of P uncorrelated sources in M parallel spaces, propagating from one space to another along the same trajectories, but with different statistics. As the time-variations of $\mathbf{J}_n$ increase (*e.g.*, very fast Doppler), the source signals become more stationary during a short observation time-interval (notice here that Eq. (9) is still necessary for power control). Contrary to the previous approach (STAR-SS), faster time-variations of $\mathbf{J}_n$ speed up the convergence since STAR-ES involves the statistics of $\mathbf{J}_n$ rather than its instantaneous realizations.

Over the m^{th} column vector of $\mathbf{Z}_n^T$ denoted by $Z_{m,n}$, define now the signal eigen-subspace by the $L \times P$ eigen-matrix, say $\mathbf{U}_m$, corresponding to the P largest eigenvalues of the correlation matrix R_{Z_m} of $Z_{m,n}$. Then for $m = 1, \cdots, M$ and $p = 1, \cdots, P$ we have $\mathcal{F}(\tau_p)^H \mathcal{U}_m \mathcal{U}_m^H \mathcal{F}(\tau_p)/L^2 = 1$, where $\mathcal{U}_m$ denotes the column-by-column FFT of $\mathbf{U}_m$. We shall use this high resolution feature to provide a localization spectrum and its root solutions similar to the previous approach, but first we need to estimate the signal eigen-matrices $\mathbf{U}_m$.

We propose an adaptive eigen-subspace tracking technique similar to [15] which can be seen as an unconstrained version of [12], but other algorithms can be used. Remember that we need an initial estimate of the signal eigen-subspace dimension P. To show the robustness of STAR-ES to this initial rank estimation problem, we define here $P_{\max} \ll L$ as the maximum number of resolvable paths that could appear simultaneously (*i.e.*, $P < P_{\max}$), and track the $L \times P_{\max}$ eigen-matrix $\hat{\mathbf{U}}_{m,n}$ for $m = 1, \cdots, M$ by:

$$\hat{\mathbf{U}}_{m,n+1} = \hat{\mathbf{U}}_{m,n} + \eta_{m,n}(Z_{m,n} - \hat{\mathbf{U}}_{m,n} Y_{m,n}) Y_{m,n}^H, \quad (13)$$

where $\eta_{m,n}$ is an adaptation step-size, possibly normalized, and $Y_{m,n} = \hat{\mathbf{U}}_{m,n}^H Z_{m,n}$. This equation is a simple approximation of a LMS version of [15] and behaves near as well as the exact solution. It converges to the $L \times P_{\max}$ eigen-matrix of R_{Z_m} corresponding to its $P_{\max}$ largest eigenvalues[5] such that $\hat{\mathbf{U}}_{m,n}^H \hat{\mathbf{U}}_{m,n} = I_{P_{\max}}$.

Once convergence is reached, we define the localization spectrum of STAR-ES by:

$$\mathcal{S}_{\text{ES}}(\tau) = \frac{1}{1 - \mathcal{F}(\tau)^H \hat{\mathcal{U}}_n \hat{\mathcal{U}}_n^H \mathcal{F}(\tau)/ML^2}, \quad (14)$$

where the $L \times (MP_{\max})$ matrix $\hat{\mathcal{U}}_n$ is the column-by-column FFT[6] of $\hat{\mathbf{U}}_n = [\hat{\mathbf{U}}_{1,n}, \cdots, \hat{\mathbf{U}}_{M,n}]$. Its root solutions are given in a way similar to STAR-SS using the following polynomial:

$$\mathcal{P}_{\text{ES}}(z) = 1 - \mathcal{F}(\tau)^H \hat{\mathcal{U}}_n \hat{\mathcal{U}}_n^H \mathcal{F}(\tau)/ML^2, \quad (15)$$

and provide $\hat{P}$ and $\hat{\tau}_1, \cdots, \hat{\tau}_{\hat{P}}$ as well as $\hat{\mathbf{D}}$. $\hat{\mathcal{U}}_n$ contains $(P_{\max} - P)$-dimensional noise eigen-subspaces. The performance in localization decreases as $(P_{\max} - P)$ increases, but still remains acceptable in practical situations.

B.3 Spatio-Temporal Separation and Reconstruction

Once $\hat{\mathbf{D}}$ is estimated, we use again the same analogy and estimate $\hat{\mathbf{J}}_n$ by multi-source beamforming [12] and compute its constituting elements $\hat{\mathbf{G}}_n$ and $\hat{\Upsilon}_n$ as follows:

$$\begin{aligned}
\hat{\mathbf{J}}_n &= \left[\hat{J}_{1,n}, \cdots, \hat{J}_{P,n}\right] = \tilde{\mathbf{H}}_n \hat{\mathbf{D}} \left(\hat{\mathbf{D}}^T \hat{\mathbf{D}}\right)^{-1}, \quad (16)\\
\hat{\mathbf{G}}_n &= \|\hat{\mathbf{J}}_n\|_F \left[\hat{J}_{1,n}/\|\hat{J}_{1,n}\|, \cdots, \hat{J}_{P,n}/\|\hat{J}_{P,n}\|\right],\\
\hat{\Upsilon}_n &= \text{diag}\left\{\left[\|\hat{J}_{1,n}\|/\|\hat{\mathbf{J}}_n\|_F, \cdots, \|\hat{J}_{P,n}\|/\|\hat{\mathbf{J}}_n\|_F\right]\right\},
\end{aligned}$$

where $\|.\|_F$ denotes the Frobinius norm of a matrix. We finally reconstruct the spatio-temporal propagation matrix $\hat{\mathbf{H}}_n = \hat{\mathbf{G}}_n \hat{\Upsilon}_n \hat{\mathbf{D}}^T$ or equivalently $\hat{\underline{\mathbf{H}}}_n$ with respect to the spatio-temporal structure of the channel in Eq. (3). The norm of propagation vectors $\sqrt{K_n}$, mentioned earlier below Eq. (6), is equal to $\|\hat{\mathbf{J}}_n\|_F = (\sum_{p=1}^{\hat{P}} \|\hat{J}_{p,n}\|^2)^{1/2}$ such that $\|\hat{\mathbf{H}}_n\|_F = \sqrt{M}$. Using Eq. (16) and Eq. (10) and assuming $\hat{\mathbf{D}} \simeq \mathbf{D}$, we can write $\hat{\mathbf{H}}_n = \mathbf{H}_n + \mathbf{E}_n \hat{\mathbf{D}} (\hat{\mathbf{D}}^T \hat{\mathbf{D}})^{-1} \hat{\mathbf{D}}^T$. Reconstruction projects the matrix of identification errors $\mathbf{E}_n$ in the source-subspace defined by $\hat{\mathbf{D}}$, and reduces its energy by a factor of L/P. It significantly improves the performance of STAR as shown next by simulations.

Once time-acquisition is made, the time-delays localization procedures described earlier, STAR-SS or STAR-ES,

[5] If R_{Z_m} can be assumed identical for $m = 1, \ldots, M$ (*e.g.*, ultra high Doppler), we can take the average of Eq. (13) over sensors in a joint eigen-subspace tracking scheme.

[6] $\hat{\mathcal{U}}_n$ could be directly estimated using Eq. (13) in the frequency domain.

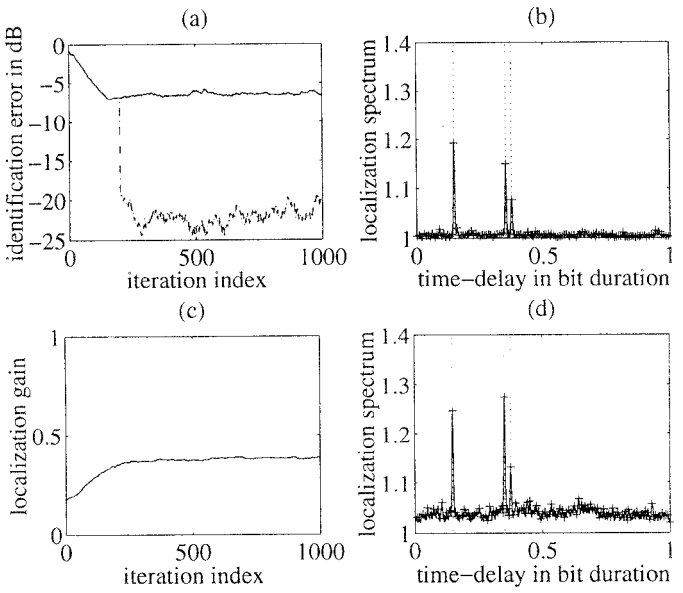

Fig. 1. $\sigma_{\mathcal{I}}^2 = 64$ and Doppler of 1Hz. (a) Identification errors in dB without spatio-temporal reconstruction (solid) and with tracking in [10] (semi-dashed). (b) Localization spectrum and its root solutions using STAR-SS. (c) Localization gain. (d) Localization spectrum and its root solutions using STAR-ES.

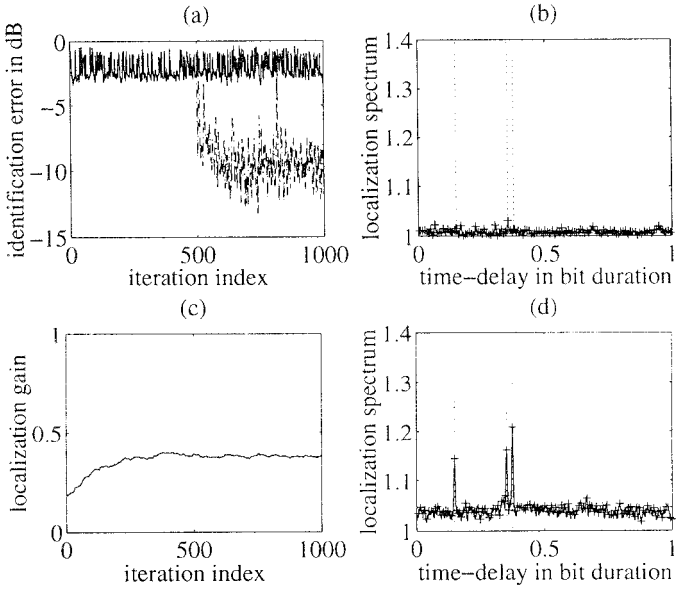

Fig. 2. $\sigma_{\mathcal{I}}^2 = 64$ and Doppler of 250Hz. (a) Identification errors in dB without spatio-temporal reconstruction (solid) and with tracking in [10] (semi-dashed). (b) Localization spectrum and its root solutions using STAR-SS. (c) Localization gain. (d) Localization spectrum and its root solutions using STAR-ES.

are replaced in [10] by a time-delays tracking algorithm. We applied in [10] an efficient angle of arrival tracking algorithm we refer to here as the adaptive source-subspace extraction and tracking (ASSET) technique (see [12] and related references therein). The ASSET algorithm optimally exploits the space manifold structure for angle of arrival tracking (see a comparative evaluation with promising methods in [16]). It was adapted to time-delays tracking in a time manifold[7] with a low computational cost and without need for permanent localization [10].

For a large processing gain, notice that we can further reduce the complexity of multipath tracking in [10] by truncating the data block $\mathbf{Z}_n$ to its $L' < L$ columns that cover the time-delay spread with a sufficient margin for the tracking. Notice finally that the formulation of STAR holds in the limiting case where the number of antennas M is 1. Hence, an application to downlink can be viewed without a pilot signal.

IV. Simulations

We consider $M = 4$ sensors, $P = 3$ paths with time-delays $\tau_1 \simeq 0.15\ T$, $\tau_2 \simeq 0.35\ T$ and $\tau_3 \simeq 0.38\ T$, a maximum number of resolvable paths $P_{\max} = 5$, and a processing gain $L = 128$. Simulations with higher values of P are not considered for lack of space, but STAR-SS as well as STAR-ES properly achieve localization. We generate 2 sets of $M \times P = 12$ uncorrelated Rayleigh fading paths at the data bit rate of 9.6 kb/s, with Dopplers of 1 Hz and 250 Hz respectively. We finally assume a perfect power control situation (*i.e.*, $\psi^2(t) = 1$, see power control capacity in [11]).

[7]We may characterize $\hat{\mathbf{G}}_n$ in a space manifold, if assumed as in [7]-[9], using the ASSET technique [12].

The estimate of the total received power $\hat{\psi}_0^2$ is initialized at 0.1, and $\hat{\underline{\mathrm{H}}}_0$ with norm $\sqrt{M}$ in (9) is started at random as well as $\hat{\mathbf{U}}_0$ in (13) whose columns are normalized to 1.

In the first scenario, the interference power $\mathcal{I}(t)$ in (1) has $\sigma_{\mathcal{I}}^2 = 64$ (*i.e.*, $SINR_{in} \simeq -18$ dB, or 3 dB after despreading) and the Doppler is 1Hz. In Fig. 1a, identification errors $|\tilde{\underline{\mathrm{H}}}_n^H \underline{\mathrm{H}}_n|/M$ (solid line) show that $\tilde{\underline{\mathrm{H}}}_n$ converges rapidly to the spatio-temporal channel within about 200 T. In Fig. 1b, the localization spectrum of STAR-SS and its root solutions, given after convergence, provide estimates of the number of paths and their time-delays with an accuracy of roughly $10^{-3}T$ [10]. The spatio-temporal reconstruction from these estimates at $n = 200$ and the multipath tracking in [10] reduce identification errors $|\hat{\underline{\mathrm{H}}}_n^H \underline{\mathrm{H}}_n|/M$ by almost $10\log_{10}(L/P) \simeq 16$ dB as expected (see Fig. 1a, semi-dashed line), and decrease the bit error rate in the considered scenario by almost a factor of 50 down to 10^{-3}. In Fig. 1c, the localization gain $(\mathrm{tr}(\mathbf{D}^H \hat{\mathbf{U}}_n \hat{\mathbf{U}}_n^H \mathbf{D})/MP)^{1/2}$ shows that STAR-ES converges at a slower rate, within about 400 T. Its localization spectrum and its root solutions in Fig. 1d show a performance in localization comparable to STAR-SS. Despite the high resolution capacity of STAR-ES, the noise present in the signal eigen-subspace as well as the low Doppler slow down its convergence and reduce its performance. In such a case, it is better to use STAR-SS whose complexity is lower.

In the second scenario we increase the Doppler to 250 Hz. In Fig. 2a, identification errors (solid line) show that $\tilde{\underline{\mathrm{H}}}_n$ fails to track the very high variations of the spatio-temporal channel. In Fig. 2b, the localization spectrum of STAR-SS and its root solutions estimated at $n = 500$ reveal none of the time-delays. The advantages of STAR-ES over STAR-SS are evident here. Fig. 2c shows that

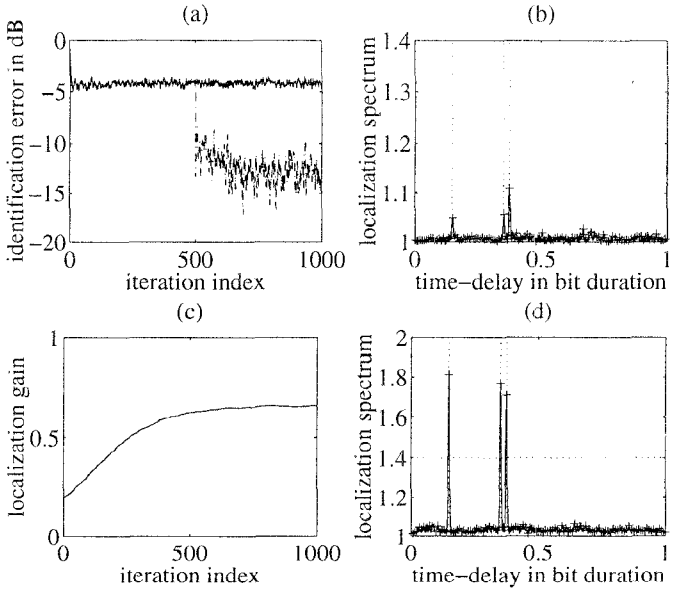

Fig. 3. $\sigma_x^2 = 16$ and Doppler of 250Hz. (a) Identification errors in dB without spatio-temporal reconstruction (solid) and with tracking in [10] (semi-dashed). (b) Localization spectrum and its root solutions using STAR-SS. (c) Localization gain. (d) Localization spectrum and its root solutions using STAR-ES.

STAR-ES still converges within 400 T despite the presence of a fast Doppler. Its localization spectrum and its root solutions in Fig. 2d show a performance comparable to the previous scenario. The spatio-temporal reconstruction from the resulting time-delay estimates is made at $n = 500$ using $\mathbf{Z}_n$ instead of $\tilde{\mathbf{H}}_n$ in (16). The multipath tracking in [10], following this step, again reduces identification errors as shown in semi-dashed line of Fig 2a, but the misadjustment increases with a faster Doppler.

In the third example, we decrease the power of interference to $\sigma_x^2 = 16$ (*i.e.*, $SINR_{in} \simeq -12$ dB, or 9 dB after despreading). In Fig. 3a, the spatio-temporal identification converges rapidly but the errors are higher. In Fig. 3b, the localization spectrum of STAR-SS and its root solutions reveal the time-delays, but the estimation with STAR-SS is not reliable in the presence of a fast Doppler, even at a lower interference level. On the other hand, Fig. 3c shows that STAR-ES has a better convergence behavior. Its performance in localization significantly improves as illustrated by its localization spectrum and its root solutions in Fig. 3d. The spatio-temporal reconstruction is again made at $n = 500$, using this time $\tilde{\mathbf{H}}_n$ in (16) as usually defined.

The table below compares performance features of STAR-SS and STAR-ES:

	STAR-SS	**STAR-ES**
convergence	fast	slow
complexity	$O(ML)$	$O(MP_{\max}L)$
accuracy	fair	high resolution
application	slow Doppler	fast Doppler

V. Conclusions

The spatio-temporal array-receiver (STAR) we proposed for asynchronous CDMA offers many advantages when compared to previous methods [1]-[4]:

- Attractive formulation: STAR formulates from the block despread data an attractive instantaneous mixture model of a narrowband source with a one-dimensional spatio-temporal channel and processes it at the bit rate. The new model called PCM (post-correlation model) allows for a structural approach to blind channel equalization and time-delays acquisition.
- Very low complexity: STAR has a very simple structure of narrowband processors, and requires only orders of $O(ML)$ and $O(MP_{\max}L)$ operations per bit for STAR-SS and STAR-ES respectively.
- High performance: STAR shows fast and accurate time-delays acquisition and tracking [10] in the presence of strong interference and fast Doppler. It optimally reduces interference by decision feedback identification (DFI) and offers a potential capacity to accommodate a larger number of users per cell [11].

References

[1] A.J. Viterbi, *CDMA Principles of Spread Spectrum Communication*, Addison-Wesley, 1995.

[2] A.F. Naguib and A. Paulraj, "Effects of multipath and base-station antenna arrays on uplink capacity of cellular CDMA", *Proc. GLOBECOM'94*, 1994, pp. 395-399.

[3] M.D. Zoltowski and J. Ramos, "Blind multi-user access interference cancellation for CDMA based PCS/cellular using antenna arrays", *Proc. ICASSP'96*, vol. 5, 1996, pp. 2730-2733.

[4] H. Liu and G. Xu, "Blind equalization for CDMA systems with aperiodic spreading sequences", *Proc. ICASSP'96*, vol. 5, 1996, pp. 2658-2661.

[5] C. Papadias and A. Paulraj, "Space-time signal processing for wireless communications", *Proc. IEEE SP Workshop on Signal Processing Advances in Wireless Communications SPAWC'97*, Paris, France, pp. 285-288, April 16-18, 1997.

[6] J. Gunther and A. Swindlehurst, "Algorithms for blind equalization with multiple antennas based on frequency domain subspaces", *Proc. ICASSP'96*, vol. 5, 1996, pp. 2421-2424.

[7] M. Wax and A. Leshem, "Joint estimation of time delays and directions of arrival of multiple reflections of a known signal", *Proc. ICASSP'96*, vol. 5, 1996, pp. 2622-2625.

[8] M. Vanderveen, C. Papadias, and A. Paulraj, "Joint angle and delay estimation (JADE) for multipath signals arriving at an antenna array", *IEEE Comm. Lett.*, vol. 1, pp. 12-14, Jan. 1997.

[9] A.-J. van der Veen, M. Vanderveen, and A. Paulraj, "SI-JADE: an algorithm for joint angle and delay estimation using shift-invariance properties", *Proc. SPAWC'97*, 1997, pp. 161-164.

[10] S. Affes and P. Mermelstein, "Spatio-temporal array-receiver for multipath tracking in cellular CDMA", *Proc. ICC'97*, vol. 3, 1997, pp. 1340-1345.

[11] S. Affes and P. Mermelstein, "Capacity improvement of cellular CDMA by the subspace-tracking array-receiver", *Proc. SPAWC'97*, 1997, pp. 233-236.

[12] S. Affes, S. Gazor, and Y. Grenier, "A subarray manifold revealing projection for partially blind identification and beamforming", *IEEE SP Lett.*, vol. 3, pp. 187-189, June 1996.

[13] R.O. Schmidt, "Multiple emitter location and signal parameter estimation", *IEEE Trans. AP*, vol. 34, pp. 276-280, March 1986.

[14] A.J. Barabell, "Improving the resolution performance of eigenstructure-based direction-finding algorithms", *Proc. ICASSP'83*, vol. 1, 1983, pp. 336-339.

[15] B. Yang, "Projection approximation subspace tracking", *IEEE Trans. SP*, vol. 43, pp. 95-107, Jan. 1995.

[16] C. Riou and T. Chonavel, "Fast adaptive eigenvalue decomposition: a maximum likelihood approach", *Proc. ICASSP'97*, vol. 5, 1997, pp. 3565-3568.